Supporting Information Section 1

S1. IV curves and noise characterization of pores formed in membranes thinned from 100 nm with a 537 pC He-ion dose

We present typical linear IV curves and 1/f noise characterization showing low to moderate 1/f noise for independent pores formed in the 250 x 250 nm^2 HIM-thinned regions of individual 100-nm thick SiN_x membranes. The pores were formed within a few hundred seconds with the application of 6 to 8 V by CBD in 3.6M LiCl (pH8).

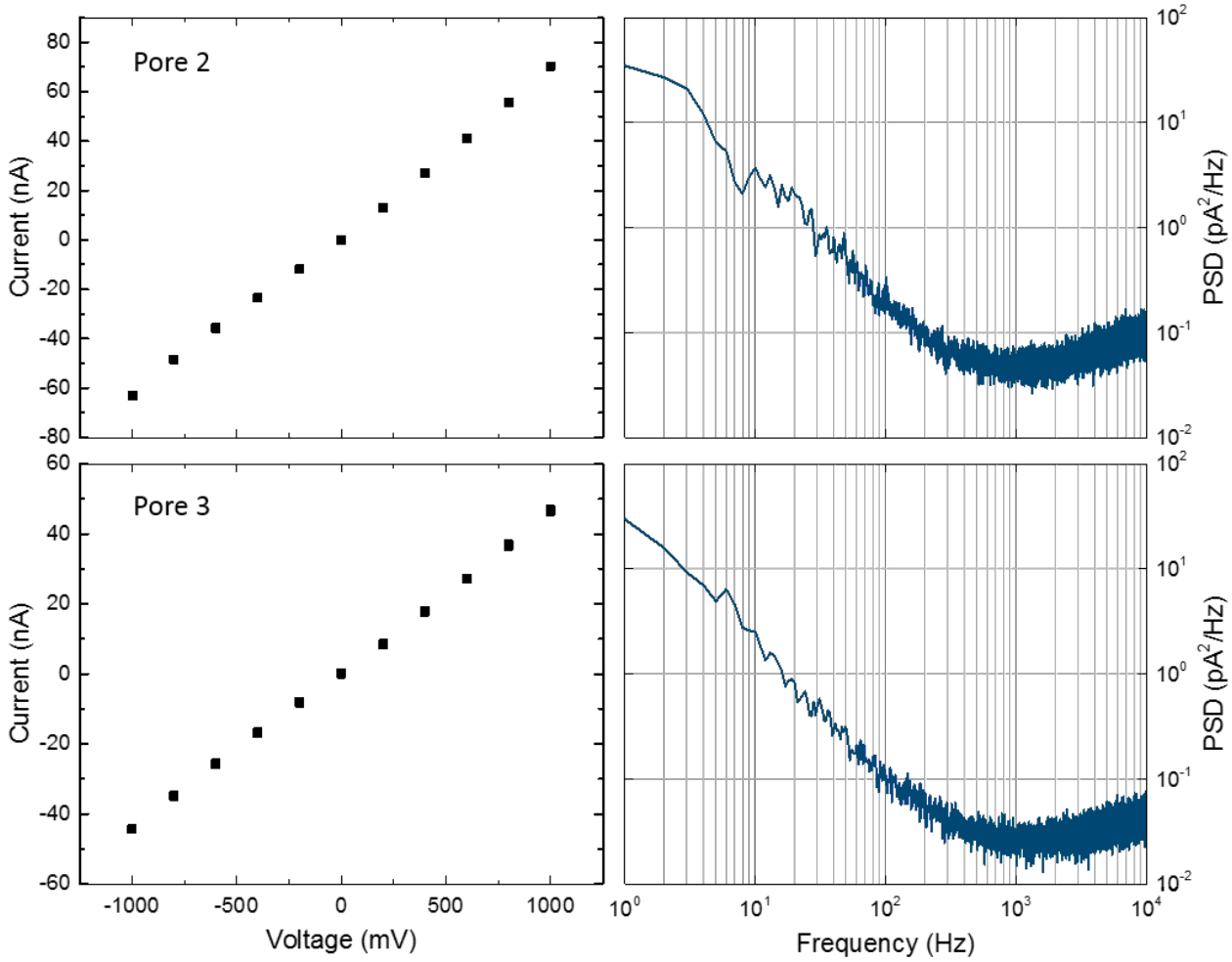

Figure S1: IV characteristics and power spectrum densities captured at 200 mV for two different nanopores formed in 100-nm thick membranes thinned to roughly 7 to 8 nm by a He-ion dose of 537 pC. Measurement performed in 3.6M LiCl (pH8) using an Axopatch 200B.

Supporting Information Section 2

S2. IV curve, noise characterization and DNA translocation data for a pore formed in a membrane thinned from 100 nm with a 586 pC He-ion dose

We present linear IV and low 1/f noise characterization (Figure S2 a,b) for a typical pore formed with a 586 pC He-ion dose in the 250 x 250 nm^2 HIM-thinned region of an individual 100-nm thick SiN_x membrane. The pore was formed with the application of 6 to 8 V by CBD in 3.6M LiCl (pH8). DNA translocations through the pore also showed unequivocally that pore formation occurred in the thinned region. The average conductance blockage was 3.2 ± 0.4 nS (Figure S2 c,d), corresponding to a thickness of 18 ± 3 nm. While this is thicker than the membranes exposed to the lower ion dose (see SI section 1), it is still a reasonable value, with the variation potentially related to the anomalous formation behavior noted in the main text.

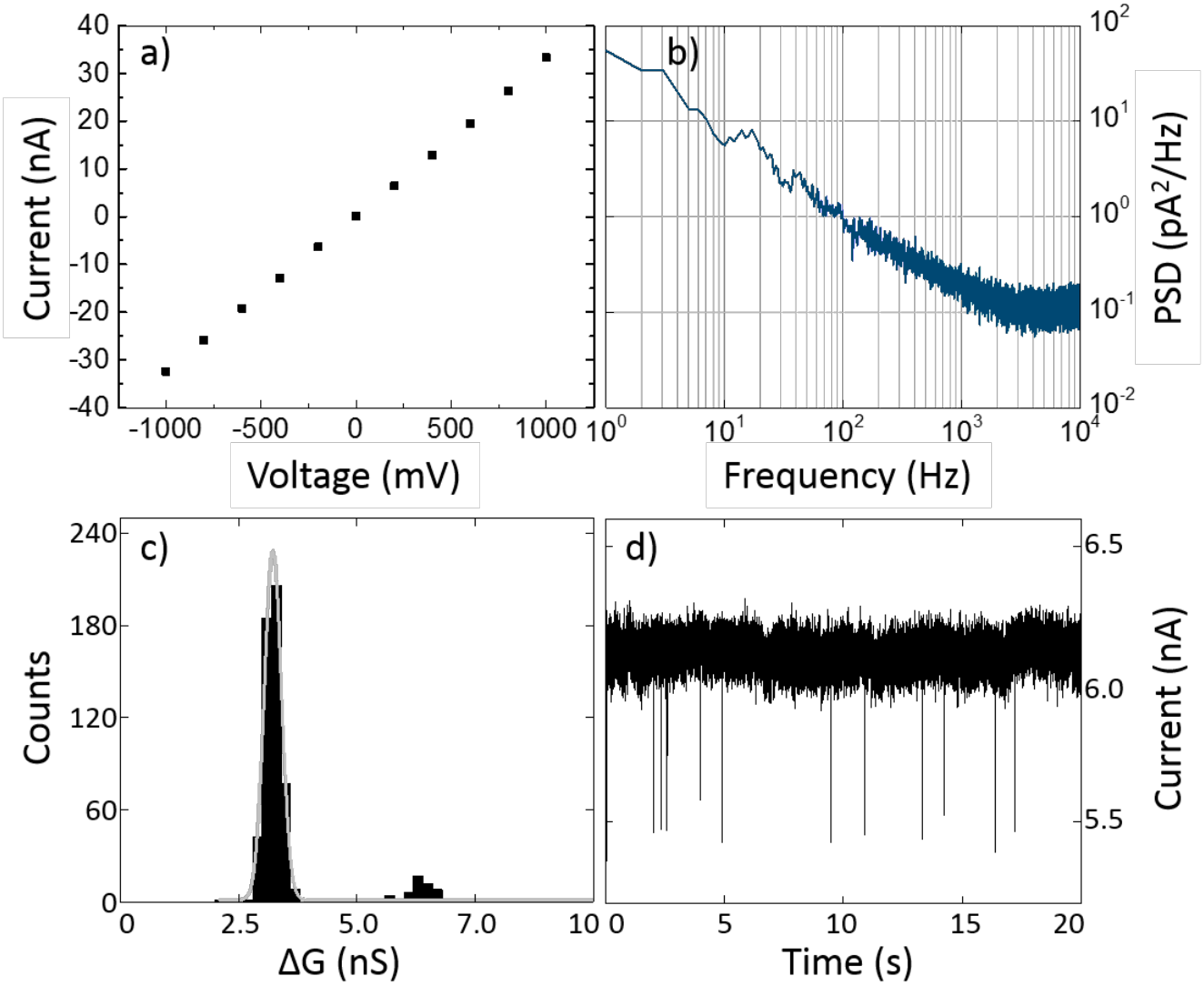

Figure S2: IV characteristics (a) and power spectral density (b) captured at 200 mV for a nanopore formed in a 100-nm thick membranes HIM-thinned by a dose of 586 pC. Conductance blockage histogram (c) with example current trace (low-pass filtered at 10 kHz) (d) for translocations of 6 nM solution of 5 kb dsDNA at 200 mV through the same pores. All measurements performed in 3.6M LiCl (pH8) using an Axopatch 200B.

Supporting Information Section 3

S3. Method of pore diameter calculation

Values for membrane thickness (L) were calculated using the simplest conductance model for a cylindrical pore:[1,2]

$$\Delta GDNA=\sigma\pi dDNA24L\ , \tag{1}$$

by substituting the 2.2 nm known diameter of dsDNA (d_{DNA}), along with the measured solution conductivity (σ = 155.6 mS/cm) and first-level blockage depth (ΔG_{DNA}). The extracted membrane thickness value was then used in a conductance model incorporating access region effects with a cylindrical pore geometry to obtain the pore diameter (d) from the measured open pore conductance (G):

$$G=\sigma 4L\pi d2+1d-1. \tag{2}$$

Supporting Information Section 4

S4. Helium bubbles in membranes thinned from 100 nm with no additional treatment

Figure S3 shows the TEM visualization of two different 100 nm thick membranes HIM-thinned with a dose of 537 pC (left) and 500 pC (right). Neither membrane had been previously subjected to cleaning, liquid immersion or voltage application. The circular features visible in the brighter thinned region likely correspond to helium-filled voids.

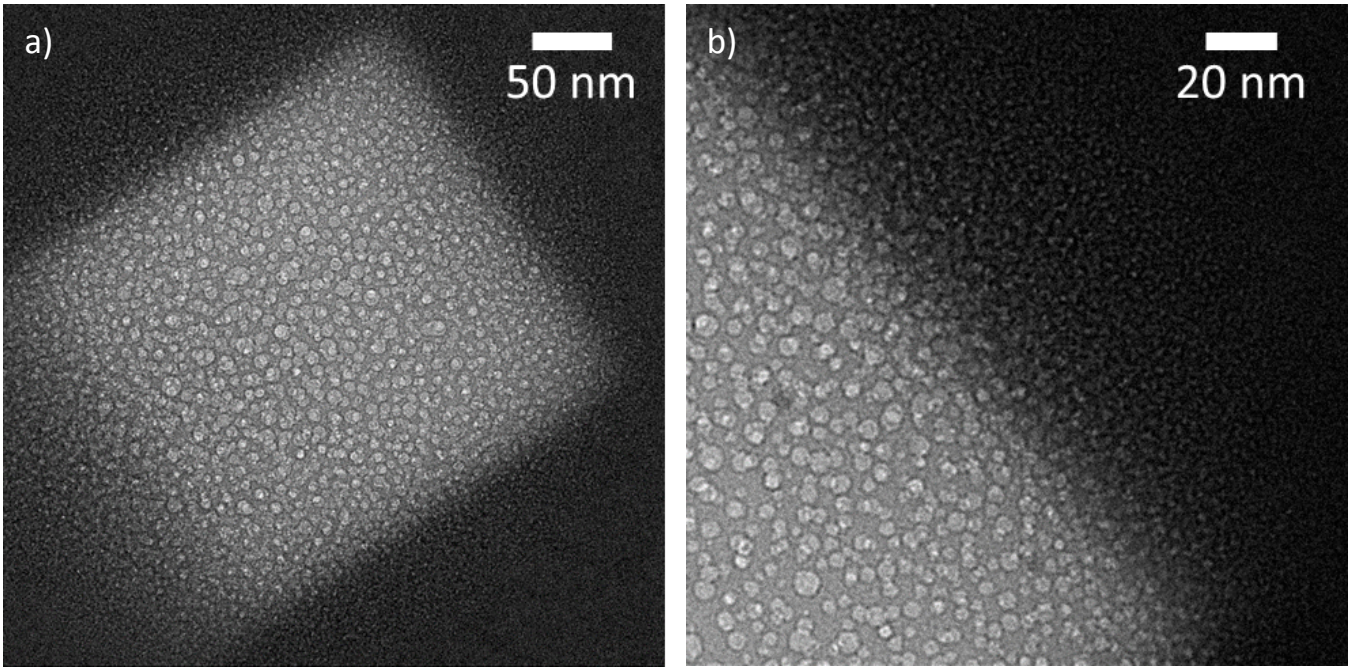

Figure S3: TEM images of helium bubbles trapped in SiN_x membranes thinned by HIM using doses of a) 537 pC and b) 500 pC.

Supporting Information Section 5

S5. DNA translocation data for a pore formed in a membrane thinned from 30 nm

We present a typical trace observed for DNA translocations through a SiN_x membrane thinned from 30 nm in a 100 x 100 nm^2 region. Following CBD-based pore fabrication at 8 V in 1 M KCl solution (pH 10), a solution of 5 kbp dsDNA in 3.6 M LiCl (pH 8) was loaded into the fluidic cell reservoir on the thinned side of the membrane. Upon application of 200 mV, we observed blockage values as shown in the trace below. The average conductance blockage value was 4.97 ± 0.08 nS, corresponding to a thickness of 12 ± 1 nm.

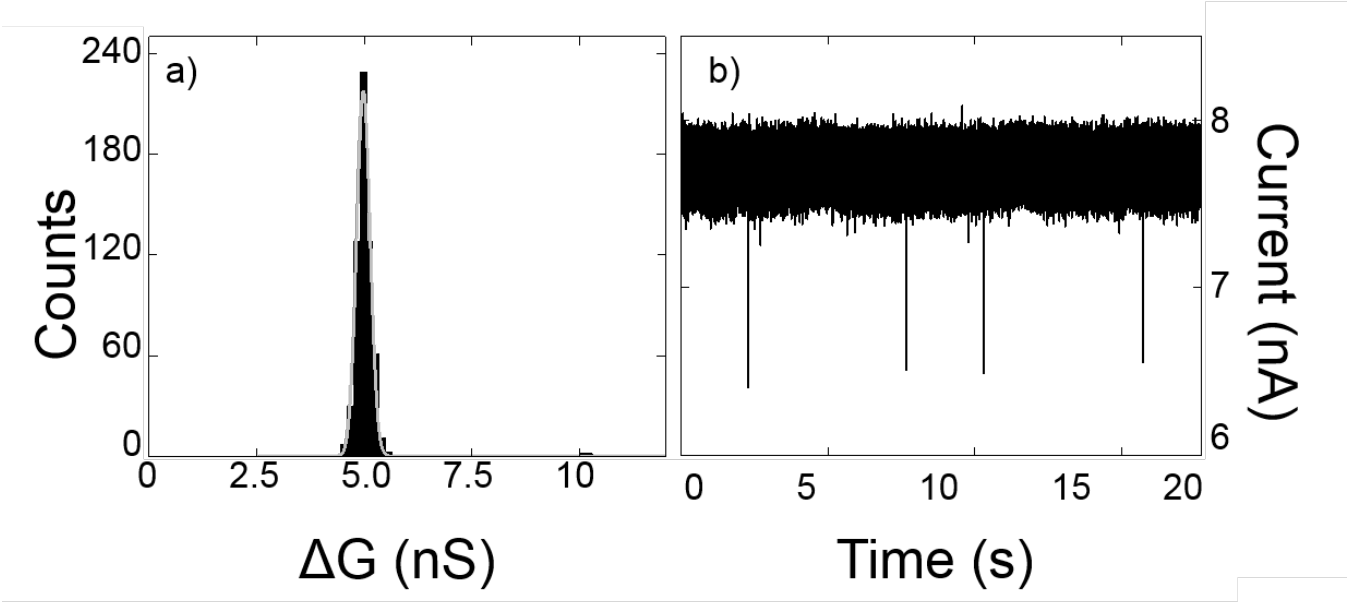

Figure S4: Conductance blockage histogram (a) with example current trace (b) corresponding to the translocation of an 11 nM solution of 5 kbp dsDNA in 3.6M LiCl (pH 8) through pore fabricated by CBD in SiN_x membrane HIM-thinned from 30 nm to roughly ~10 nm. Data low-pass filtered at 100 kHz.

Supporting Information Section 6

S6. TEM images of pores in membranes thinned from 30 nm

We performed TEM on SiN_x membranes thinned from 30 nm with a He-ion dose of 32 pC. Unlike the membranes exposed to 537 or 586 pC He-ion doses, these membranes did not display circular features in the thinned regions. Further, the pores clearly appeared in the square thinned (brighter) region, confirming effective pore localization through thinning by just 25 to 60%. Pores were formed by CBD at 8V in 1 M KCl (pH 10). Dark areas are most likely salt residues left over from the drying process. Minimal cleaning was performed between pore fabrication and TEM imaging in order to avoid potential changes to the nanopore. (Note that the bright circular features evident in 100-nm-thick films that have been thinned with larger He-ion dose are not visible in either case.)

Translocation of dsDNA at 200 mV in 3.6 M LiCl (pH 8) produced average conductance blockage values of 2.6 ± 0.9 nS (pore 9) and 4 ± 1 nS (pore 11). These values correspond to respective membrane thicknesses of 23 ± 8 nm and 13 ± 4 nm, compared to an original membrane thickness of 30 nm.

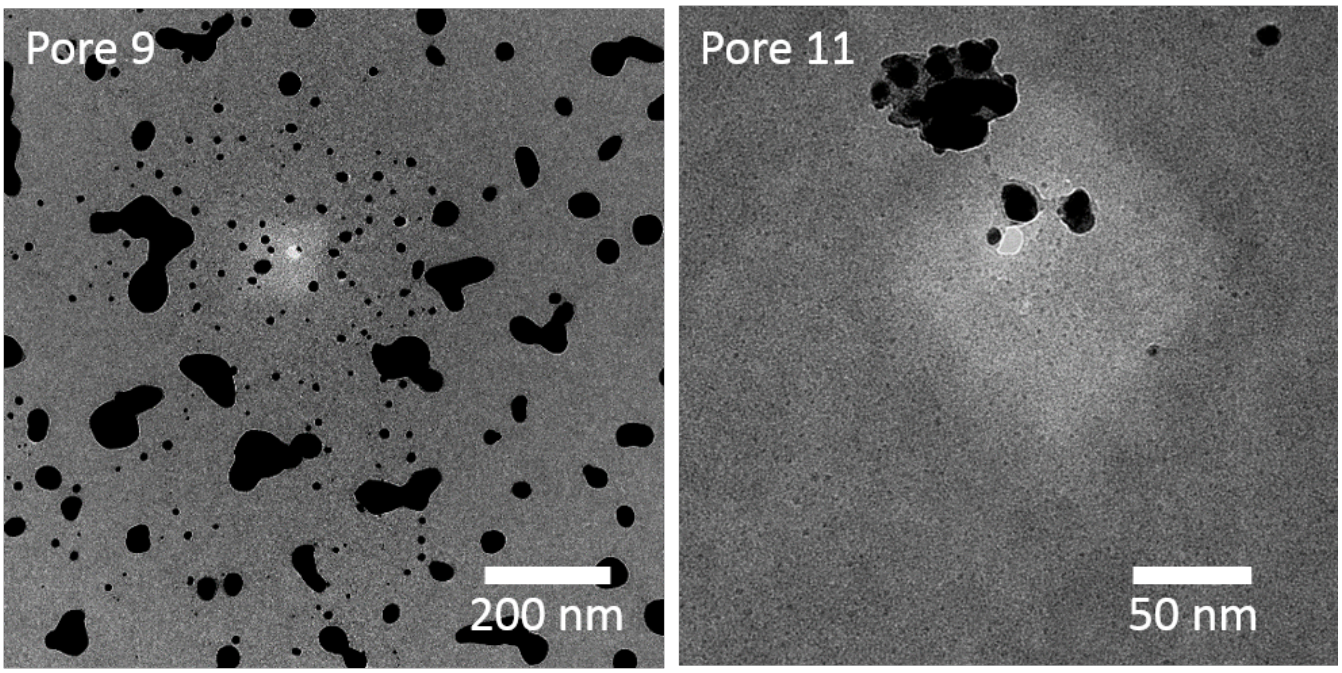

Figure S5: TEM images show a pore appearing in the 100 x 100 nm^2 regions thinned to ~23 nm (pore 9) and ~13 nm (pore 11) from an original 30-nm SiN_x thickness.

[1] Smeets R M M, Keyser U F, Krapf D, Wu M-Y, Dekker N H and Dekker C 2006 Salt dependence of ion transport and DNA translocation through solid-state nanopores. *Nano Lett.* **6** 89–95

[2] Kowalczyk S W, Grosberg A Y, Rabin Y and Dekker C 2011 Modeling the conductance and DNA blockade of solid-state nanopores. *Nanotechnology* **22** 315101

[3] Beamish E, Kwok H, Tabard-Cossa V and Godin M 2012 Precise control of the size and noise of solid-state nanopores using high electric fields. *Nanotechnology* **23** 405301

[4] Neri B, Olivo P and Riccò B 1987 Low-frequency noise in silicon-gate metal-oxide-silicon capacitors before oxide breakdown *Appl. Phys. Lett.* **51** 2167

[5] Sakura T, Utsunomiya H, Kamakura Y and Taniguchi K 1998 A detailed study of soft- and pre-soft-breakdowns in small geometry MOS structures *International Electron Devices Meeting 1998. Technical Digest (Cat. No.98CH36217)* (IEEE) pp 183–6

[6] Jackson J C, Robinson T, Oralkan O, Dumin D J and Brown G A 1998 Differentiation Between Electric Breakdowns and Dielectric Breakdown in Thin Silicon Oxides *J. Electrochem. Soc.* **145** 1033

[7] Roussel P, Degraeve R, Van den Bosch C, Kaczer B and Groeseneken G 2001 Accurate and robust noise-based trigger algorithm for soft breakdown detection in ultra thin oxides *2001 IEEE International Reliability Physics Symposium Proceedings. 39th Annual (Cat. No.00CH37167)* (IEEE) pp 386–92

[8] Schmitz J, Tuinhout H P, Kretschmann H J and Woerlee P H 2001 Comparison of soft-breakdown triggers for large-area capacitors under constant voltage stress *IEEE Trans. Device Mater. Reliab.* **1** 150–7